

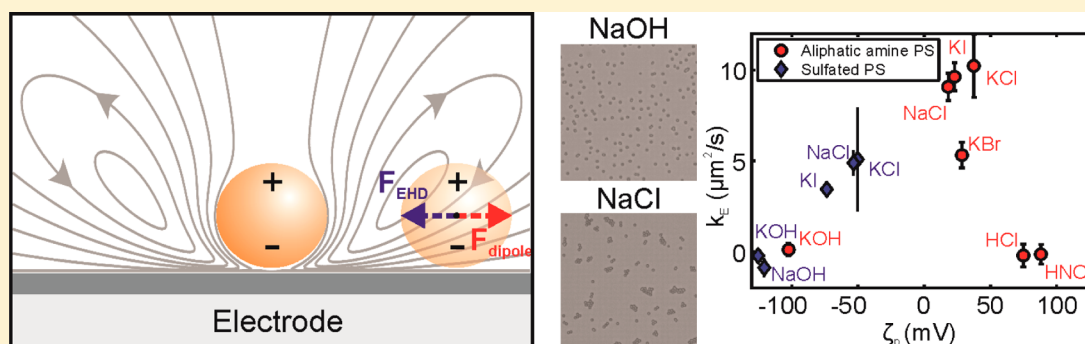
Electrolyte-Dependent Aggregation of Colloidal Particles near Electrodes in Oscillatory Electric Fields

Taylor J. Woehl,[†] Kelley L. Heatley,[†] Cari S. Dutcher,^{†,‡} Nicholas H. Talken,[†] and William D. Ristenpart^{*,†}

[†]Department of Chemical Engineering and Materials Science, University of California—Davis, Davis, California 95616, United States

[‡]Air Quality Research Center, University of California—Davis, Davis, California 95616, United States

Supporting Information



ABSTRACT: Colloidal particles adjacent to electrodes have been observed to exhibit drastically different aggregation behavior depending on the identity of the suspending electrolyte. For example, particles suspended in potassium chloride aggregate laterally near the electrode upon application of a low-frequency (~ 100 Hz) oscillatory electric field, but the same particles suspended in potassium hydroxide are instead observed to separate. Previous work has interpreted the particle aggregation or separation in terms of various types of electrically induced fluid flow around the particle, but the details remain poorly understood. Here we present experimental evidence that the aggregation rate is highly correlated to both the particle zeta potential and the electric field amplitude, both of which depend on the electrolyte type. Measurement of the aggregation rate in 26 unique electrolyte–particle combinations demonstrates that the aggregation rate decreases with increasing zeta potential magnitude (i.e., particles with a large zeta potential tended to separate regardless of sign). Likewise, direct measurements of the oscillatory electric field in different electrolytes revealed that the aggregation rate was negatively correlated with solution conductivity and thus positively correlated with the field strength. We tested the experimentally measured aggregation rates against a previously developed point dipole model and found that the model fails to capture the observed electrolyte dependence. The results point to the need for more detailed modeling to capture the effect of electrolyte on the zeta potential and solution conductivity to predict fluid flow around colloids near electrodes.

INTRODUCTION

Micrometer-sized colloidal particles have been widely observed to form planar aggregates near an electrode surface in response to an ac electric field applied normal to the electrode.^{1–18} This aggregation was originally considered to be counterintuitive because each particle has similar surface charge and dielectric properties, so assemblies of particles will experience repulsive forces due to Coulombic and dipole–dipole interactions. Because of the clearly long-range nature of the attraction, the aggregation was initially interpreted in terms of an electrohydrodynamic (EHD) fluid flow (also known as induced-charge electroosmotic flow^{19–21}) induced by each colloidal particle near the electrode surface.^{2,4,6,11,22} Trau et al. proposed that the presence of the particle perturbs the otherwise constant electric field near the electrode, creating a tangential electric field and corresponding EHD fluid flow directed toward the particle; nearby particles become mutually entrained in the

flow, and aggregation ensues.^{2,4} Ristenpart et al. further elaborated this model via a scaling analysis that treated the particles as point dipoles.¹¹ The model predicted that the EHD flow magnitude and corresponding aggregation rate should scale as the square of the applied ac electric field, and approximately inversely with frequency; this E^2 dependence is consistent with the observed aggregation under ac polarization. These scaling predictions have been corroborated experimentally via measurements of the aggregation rate of colloidal latex particles for varying applied potential and frequency.^{9,11,23}

Although the point dipole EHD model captures the effect of the electric field on the observed rate of aggregation, to date the model has had a shortcoming: it did not appear to explain the

Received: December 18, 2013

Revised: March 5, 2014

Published: April 7, 2014

Table 1. Previous Reports of Electrolyte-Dependent EHD Aggregation/Separation

electrolyte	ionic strength (mM)	particle diameter (μm)	frequency (Hz)	pairwise/multiparticle	particle behavior	ref
KCl	0.15, 1.0	2.7, 4.2, 5.7	100–4000	pairwise, multiparticle	aggregation	11, 13, 14, 8
NaCl	0.1, 1	2, 9.7	50–2000	pairwise, multiparticle	aggregation	9, 18
NaHCO ₃	0.1, 0.15	5.7, 9.7	50–1000	pairwise, multiparticle	aggregation	9, 13, 14, 16
NaN ₃	not provided	1, 2	<1000	multiparticle	aggregation	5
NH ₄ OH	0.15	5.7	100	pairwise	no motion	13
H ₂ CO ₃	0.15	5.7	100	pairwise	separation	13
KOH	0.15, 1.0	5.7, 9.7	50–100	pairwise, multiparticle	separation	9, 13, 14, 16
NaOH	0.1, 0.15, 1.0	9.7	10–1000	pairwise	separation	9, 13

observed effect of the suspending electrolyte.^{12,15,17} Specifically, multiple researchers have observed that the choice of electrolyte has a huge effect on the aggregation rate; particles are even observed to separate strongly rather than aggregate in electrolytes such as potassium hydroxide and sodium hydroxide.^{5,8,9,11,13,14,16,18} A comprehensive list of previously observed electrolyte-dependent particle aggregation/separation is shown in Table 1. A key feature of this table is that there is no obvious trend with respect to which electrolytes yield aggregation or separation. Kim et al. originally showed that particle pairs separated in 0.1 mM NaOH and KOH solutions and initially attributed the separation behavior to electrode reactions and the transference number of the electrolyte,^{6,9} however, further work showed that aggregation was not correlated with the transference number.²⁴ Additionally, Kim et al. concluded that the zeta potential of the particles did not have a significant effect on the particle behavior in ac electric fields, at least for the range of particle zeta potentials they examined (e.g., between -55 and -15 mV for particle aggregation).

Fagan et al. continued work on particle pair dynamics¹² and conducted direct measurements of the particle height over the electrode using total internal reflection microscopy (TIRM).^{24,25} By measuring the height of individual particles in each electrolyte using TIRM, Fagan et al. determined that whether the particles separated or aggregated was correlated with the electrolyte-dependent phase angle between the oscillating particle height and electric field.^{12,26} Particles with phase angles greater than 90° were observed to undergo lateral aggregation, whereas particles with phase angles of less than 90° were observed to separate. Fagan et al. developed a model to calculate the drift rate of two isolated particles in various electrolytes based on electroosmotic flow on the particle surface (ECEO), faradaically coupled electroosmotic (FCEO) flow on the electrode due to electrochemical reactions, and induced dipolar repulsion between adjacent particles.¹² The origin of the electrolyte dependence in Fagan's model is the electrolyte-dependent FCEO flow on the electrode, which causes asymmetries in the ECEO fluid flow on the particle surface leading to either aggregation or separation of the colloidal particles. Fagan's model interprets particle separation and aggregation in terms of the $O(E)$ ECEO fluid flow on the particle surface; because the particle height is also oscillating with the electric field, the direction of the ECEO flow that the particle feels at the top of its oscillation (when it is farthest from the electrode and has the highest mobility) determines whether it will aggregate with or separate from a neighboring particle. To capture this effect quantitatively, Fagan's model invoked a phase-angle-dependent ECEO fluid flow on the particle surface: for particle-current phase angles of less than 90° , the particle feels a predominantly repulsive ECEO flow at the top of its

oscillation and vice versa for phase angles greater than 90° . The model was qualitatively consistent with their observations of the aggregation and separation of particles in various electrolytes. Hoggard et al. extended the experimental observations of electrolyte-dependent particle behavior to more electrolytes¹³ and multiparticle systems,¹⁴ which corroborated previous work on particle pair dynamics.⁹ However, Wirth et al. showed that the electrolyte-dependent phase angle persisted in the absence of electrochemical reactions, suggesting that the FCEO flow in Fagan's model was not the sole source of the symmetry breaking that led to the particle-current phase angle.¹⁶ Most recently, Wirth et al. solved the standard electrokinetic model numerically and predicted phase angles that qualitatively agreed with the experimental values at some frequencies.^{16,17} They suggested that the two effects leading to electrolyte-dependent particle aggregation and separation were the electrolyte-dependent complex dynamic electrophoretic mobility and the electrolyte-dependent electric field strength.

Although Sides and Prieve and co-workers have convincingly demonstrated experimentally that the phase angle is correlated with aggregation versus separation, key questions remain. Specifically, an important aspect of the particle drift model is that the direction of the fluid flow that the particle feels at the top of its oscillation reverses for phase angles of less than 90° , resulting in the particle feeling a predominantly repulsive drag force.^{12,16} Notably, there is no direct evidence that the flow direction is actually reversed in electrolytes where separation occurs: what is observed experimentally is simply that the particles separate. The separation could indeed result from a reversal in the flow direction, but an alternative explanation that must be considered is that the flow direction actually remains unchanged and a repulsive interaction simply becomes dominant.

This possible interpretation is especially pertinent given that induced dipolar forces between particles are known to influence tremendously the particle behavior near the electrode, contributing to the formation of colloidal binary superlattices,¹⁰ wormlike structures,^{7,14,27} aggregates with large interparticle separations,¹⁴ and colloidal dimers²⁸ and molecules.²⁹ For two identical particles in a plane orthogonal to the applied field, the dipolar interaction is always repulsive and scales as $F_{\text{dipole}} \sim C_0^2 E_0^2$, where C_0 is the particle dipole coefficient. Although dipolar forces presumably affect the observed aggregation rate, their exact role and the effect of the electrolyte identity on both the dipolar interactions and the electrically generated fluid flow have remained unclear.

In this article, we experimentally measured the aggregation rate of 26 different electrolyte–particle combinations, all at 1 mM ionic strength, when subjected to a 100 Hz ac electric field. We also directly measured the ac electric field strength and zeta

potential of the particles in each electrolyte. In contrast to a previous report,⁹ we find that the aggregation rate decreases strongly with increasing zeta potential magnitude (i.e., the higher the zeta potential magnitude, the slower the particles aggregated). Likewise, we found that the aggregation rates were positively correlated with the experimentally measured electric field strengths. We tested the aggregation rate data against the point dipole EHD model, combining Ristenpart et al.'s scaling analysis¹¹ and Hinch's model for the effect of the zeta potential on the particle dipole coefficient,³⁰ but found that the point-dipole model fails to capture the observed dependence on the zeta potential. The results shed new light on the effect of electrolyte on particle aggregation near electrodes and point to the need for more detailed modeling that includes the effect of electrolyte type on both the zeta potential and electric field magnitude.

EXPERIMENTAL METHODS

The experimental methods are similar to those presented by Ristenpart et al.¹¹ The experimental apparatus (Figure 1) consisted

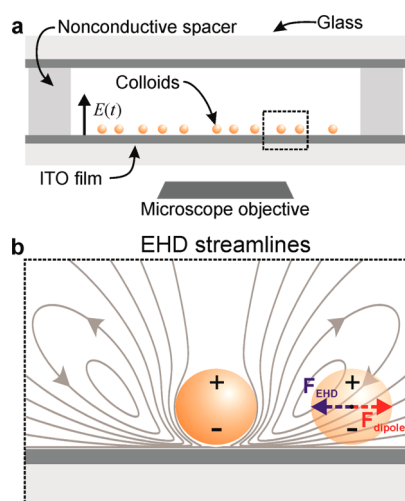


Figure 1. Schematic of (a) the experimental setup and (b) EHD flow streamlines and force vectors for the EHD drag force and induced dipolar repulsion (not to scale).

of two glass slides coated with tin-doped indium oxide (ITO, 5–15 Ω) separated by a 1-mm-thick nonconductive poly(dimethylsiloxane) spacer. Prior to each experiment, the electrodes were washed with soap and water, then ultrasonicated in acetone and DI water for 10 min each, and finally dried with filtered compressed air. Stock solutions of each electrolyte were prepared at a concentration of 1 mM using Millipore-grade DI water (18.2 M Ω cm). We restricted our study to 1:1 monovalent electrolytes to keep the Debye length constant at \sim 10 nm. Colloidal suspensions using various electrolytes were made by adding either 4- μ m-diameter silica particles (Polysciences), 2- μ m sulfated polystyrene (PS) (Invitrogen), or 2- μ m aliphatic amine PS (Invitrogen) to the desired electrolyte at a volume fraction of 5×10^{-6} ; each suspension was washed at least three times by centrifugation and resuspension. The zeta potential of each colloidal suspension was measured using dynamic light scattering (Zetasizer, Malvern Instruments Ltd.). Refer to the Supporting Information for the relevant particle and electrolyte properties (Table S1).

To begin an experiment, the colloidal suspension was added to the fluid well, and the particles were allowed to settle by gravity to the bottom electrode. The negatively charged silica and sulfated polystyrene particles remained separated from the negatively charged ITO by colloidal scale forces (i.e., double-layer repulsion). In contrast, the positively charged aliphatic amine particles tended to adhere

irreversibly to the ITO upon contact. To prevent adhesion, an 800 mV dc bias was applied to the cell during the sedimentation period. This small dc bias provided an electrostatic “bumper” that prevented adhesion but had little other observable effect on the particles, which remained separated from the electrode and were observed to continue moving by Brownian motion.

After the particles were adjacent to the electrode, an ac potential was applied to the cell with a function generator. The resulting particle behavior was observed with a reflection microscope and recorded at 15 images per second with a digital camera. For all 4 μ m silica experiments, an ac potential of 5 V peak-to-peak (V_{pp}) and 100 Hz was used; for all 2 μ m PS experiments, an ac potential of 2 V_{pp} and 100 Hz was used. The 800 mV dc bias for the positive PS particles was removed immediately prior to application of the ac field. For a typical experiment, we recorded the particle behavior for 15 s prior to application of the electric field to establish an average number of particles and then recorded for approximately 30 s following electric field application. The field was then removed (and dc bias reapplied if using amine PS), and the particles were allowed to disperse via Brownian motion for 10–15 min before repeating the experiment. Three trial replicates were performed for each electrolyte–particle combination.

The ac electric field magnitude of each electrolyte suspension was directly measured using a high-precision electrometer (Keithley Instruments Inc.), which measured the current with a sampling frequency of 50 000 Hz. An ac potential was applied to each cell for 2 to 3 s, and the amplitude of the measured ac current was averaged over 100–200 periods; currents on the order of milliamps were typically recorded through the experimental cells. The average current was then divided by the electrode area and the conductivity of the electrolyte to yield the ac electric field magnitude. The measured amplitude of the ac electric fields is of the same order of magnitude as predicted by simply dividing the applied potential by the cell thickness ($E = 5 \text{ V}/1000 \mu\text{m} = 5 \text{ kV/m}$). Note that the electrolytes with higher conductivities tended to yield relatively lower field strengths (Figure S1, Table S1).

RESULTS AND DISCUSSION

Electrolyte-Dependent Aggregation Experiments.

Consistent with prior observations, the identity of the suspending electrolyte affected both the quantitative and qualitative behavior of the colloidal particles upon application of the oscillatory electric field. Figure 2 shows representative time-lapse images of particle behavior in different electrolytes, demonstrating the three main qualitative behaviors observed during experimentation: strong separation (Figure 2a), weak separation (Figure 2b), and strong aggregation (Figure 2c). Figure 2a shows that silica particles in NaOH separated strongly within the first 2 s of electric field application and continued to separate more slowly over the next several seconds (e.g., the particles outlined in red). In contrast, a weak separation of particles was observed for the silica in NH₄OH with little observable change in particle positions other than those imparted by Brownian motion (Figure 2b). Finally, Figure 2c shows the rapid aggregation of particles suspended in NaCl. Single particles formed planar aggregates on the surface of the electrode within seconds; the aggregates remained mobile throughout the experiment and were dispersed by Brownian motion when the electric field was removed. We emphasize that the particle type, applied electric potential and frequency, and ionic strength were identical in all three trials shown in Figure 2; the only difference was in the type of electrolyte (and parameters whose magnitude depends on the electrolyte type, cf. Table S1). Similar aggregation or separation was observed in all 26 measured electrolyte–particle combinations, with only the apparent rate of aggregation changing between electrolytes.

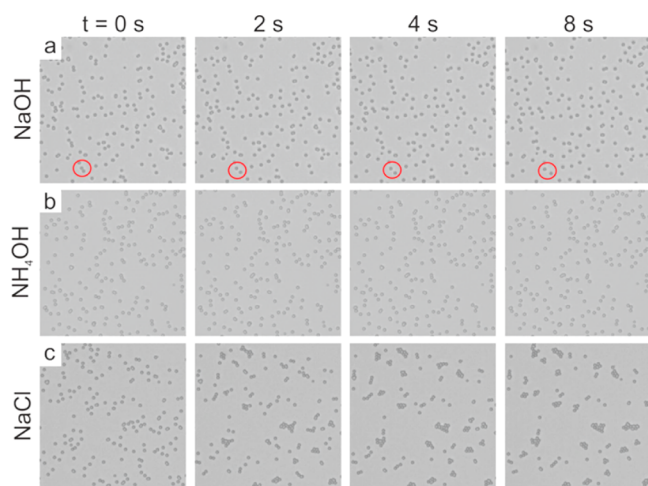


Figure 2. Representative examples of the electrolyte-dependent behavior of 4 μm silica particles upon application of an electric field (5 Vpp, 100 Hz, oriented out of the page). The electric field is applied at $t = 0$ s. (a) Strong separation of colloidal silica particles suspended in 1 mM NaOH. (b) Weak separation of particles suspended in 1 mM NH_4OH . (c) Strong aggregation of particles suspended in 1 mM NaCl.

To quantify the aggregation and separation behavior of particles in each electrolyte, we employed the singlet tracking methodology developed by Ristenpart et al. in which the number n_1 of unaggregated particles (singlets) is tracked versus time.¹¹ Assuming that the loss of singlets is dominated initially by singlet–singlet aggregation events allows the process to be modeled as a second-order kinetic reaction, yielding

$$\frac{n_1^0}{n_1} = 1 + k_E n_1^0 t \quad (1)$$

where n_1^0 is the initial concentration of singlets prior to applying the electric field, t is time, and k_E is the aggregation rate “constant” which depends on the magnitude of the attractive force pulling the singlets together. Using standard image analysis techniques, we determined the number of singlets as a function of time. Representative singlet concentrations versus time are shown in Figure 3a. The number of singlets in NaOH increased rapidly by roughly 25% after the electric field was applied and then plateaued over the next 15 s, while in NH_4OH the number of singlets increased gradually over 15 s. In contrast, strong aggregation in NaCl was commensurate with a rapid decrease in the number of singlets, in this case ultimately decaying to approximately 15% of the original number of singlets. To quantify each aggregation rate, we made use of eq 1 and fit the inverse singlet concentration versus time. An example of this procedure is shown in Figure 3b for NaCl, NaF, and NH_4OH . The inverse number of singlets for each aggregating electrolyte increased approximately linearly for the first 5–10 s and then became nonlinear due to aggregate–singlet and aggregate–aggregate collisions. On the other hand, the inverse number of singlets decreased slightly with time in NH_4OH , commensurate with particle separation increasing the total number of singlets. The effective aggregation rate constant k_E was then extracted from the initial slope of the inverse singlet concentration. To ensure that the extracted aggregation rate was dominated primarily by singlet–singlet aggregation as assumed in eq 1, the slope was determined via linear regression for $t < 10$ s or $(n_1^0/n_1) < 5$, whichever occurred first. Note that

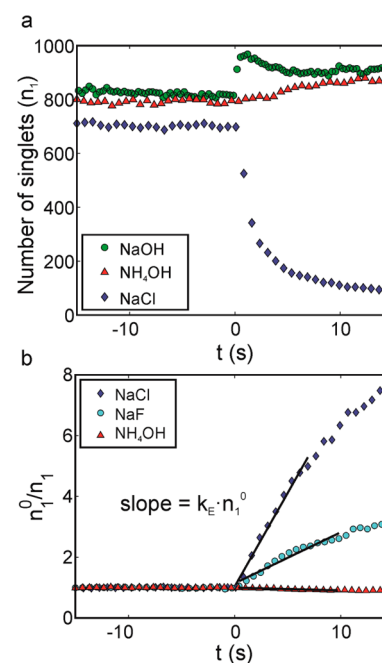


Figure 3. Quantification of the aggregation rate (k_E) of colloidal particles suspended in various electrolytes. (a) Number of singlets (n_1) as a function of time for 4 μm silica particles suspended in the three representative electrolytes shown in Figure 2. (b) Inverse number of singlets, normalized by the average number of singlets for $t < 0$ s (n_1^0), for 4 μm silica particles in three electrolytes as indicated. The black lines are least-squares fits to the initial linear regime ($t < 10$ s or $n_1^0/n_1 < 5$).

the larger k_E is, the higher the observed rate of aggregation is; for electrolytes where separation occurs, k_E is negative. The slope of the inverse number of singlets clearly increases with the aggregation rate of the particles, in this case, $k_{E,\text{NaCl}} > k_{E,\text{NaF}} > k_{E,\text{NH}_4\text{OH}}$. While the analogy of a second-order reaction breaks down for $k_E < 0$, this approach provides a single succinct metric that indicates whether particles aggregate or separate.

This procedure was repeated for all 26 electrolyte/particle combinations, with at least 3 trial replicates per combination. The results summarized in Figure 4 exhibit several noteworthy trends. First, our results are qualitatively consistent with previous reports of the effect of electrolyte on aggregation or separation (cf. Table 1): particles suspended in KOH and NaOH strongly separated, particles in NH_4OH weakly separated, while particles suspended in NaCl, KCl, and NaN_3 aggregated rapidly. Our work also clarifies the effect of several previously untested electrolytes. For example, KBr induced the fastest aggregation of any electrolyte tested for the silica particles, while LiOH induced separation behavior similar to that of KOH and NaOH. Most intriguingly, aliphatic amine PS particles separated strongly in acidic electrolytes (HCl and HNO_3) as well as hydroxide salts (i.e., KOH, Figure 4b). This result strongly indicates that the separation behavior is not solely due to high pH or some other aspect associated with hydroxide ions.

Figure 4 also suggests that the silica particles aggregated much more rapidly than the polystyrene particles: k_E was on the order of 100 $\mu\text{m}^2/\text{s}$ for the silica particles, whereas k_E was on the order of 10 $\mu\text{m}^2/\text{s}$ for both the positively and negatively charged polystyrene particles. Note, however, that both the particle size and the applied electric potential differed between

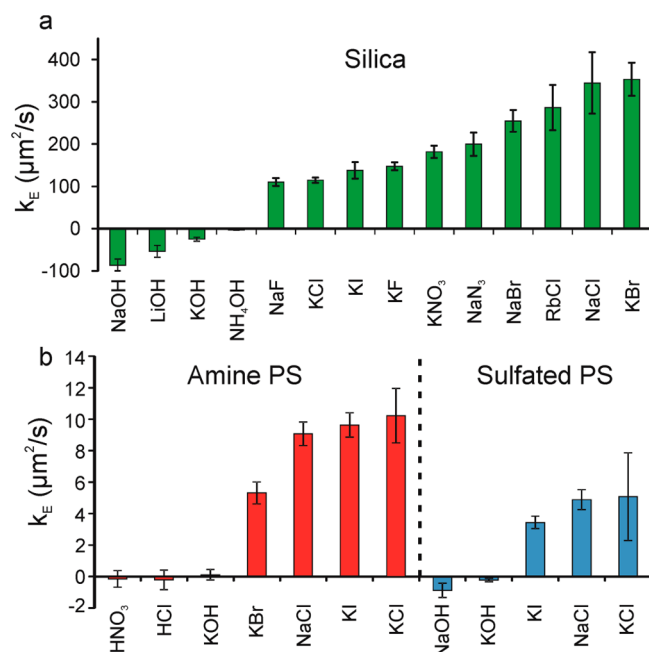


Figure 4. Aggregation rate constant (k_E) for different electrolyte/particle combinations, all at 1 mM ionic strength and 100 Hz applied frequency. (a) 4 μm silica particles at 5 Vpp. (b) 2 μm amine (red) and 2 μm sulfated (blue) PS, both at 2 Vpp. The error bars are 2 standard deviations of the mean of three trial replicates.

the two particle types (the silica was 4 μm compared to 2 μm for polystyrene, and the applied potential was 5 Vpp for silica versus 2 Vpp for both polystyrenes). The combination of a larger particle size and a larger applied field strength increased the effective aggregation rate for the silica particles; the key point here is the effect of electrolyte type for each particle type.

Effect of the Particle Zeta Potential on the Aggregation Rate. A key advantage of the data set summarized in Figure 4 is that it provides a broad sample size with which to search for correlations with various system parameters to elucidate the effect of electrolyte type. Of particular interest is the effect of the particle zeta potential. Previous observations by Kim et al. suggested that the zeta potential had a negligible effect on the behavior of pairs of colloidal particles in ac electric fields, albeit over a smaller range of zeta potentials than examined here.⁹ Our results reveal a pronounced and perhaps surprising trend: the aggregation rate was negatively correlated with the magnitude of the particle zeta potential, which varied considerably from electrolyte to electrolyte (cf. Table S1). In general, the aggregation rate decreased with the magnitude of the zeta potential for all particle types tested, regardless of sign (Figure 5). For the silica particles (Figure 5a), hydroxide electrolytes engendered zeta potentials approximately 3 times larger than the rest of the electrolytes, presumably due to increased dissociation of surface groups at high pH. All of the silica particles that aggregated had zeta potentials greater than approximately -50 mV, while those that separated had zeta potentials of less than -120 mV. A similar trend was observed for the sulfated PS particles, whose zeta potential also varied with electrolyte type due to increased dissociation of sulfonate surface groups at high pH (Figure 5b, blue diamonds). For aliphatic amine PS particles, in contrast, electrolytes with $\text{pH} < 7$ caused the dissociation of the amine surface groups, resulting in positive zeta potentials, while

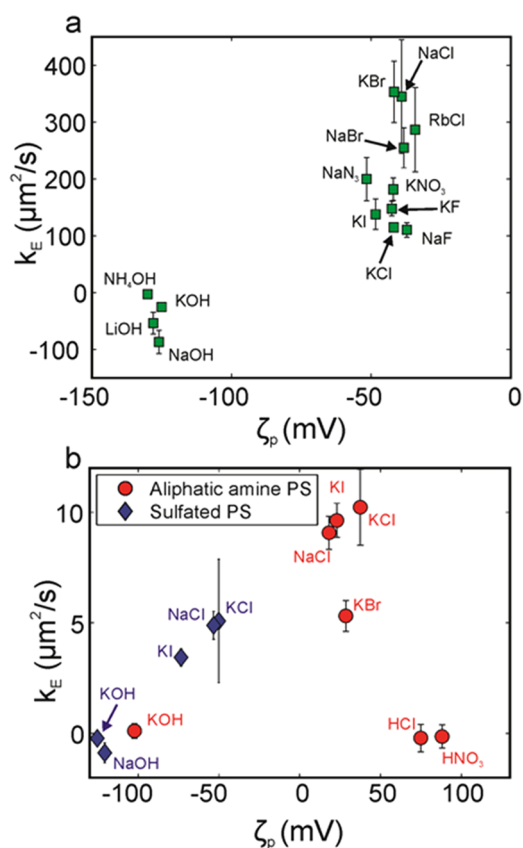


Figure 5. Aggregation rate as a function of zeta potential for (a) 4 μm silica particles and (b) 2 μm PS particles. Each point represents a different electrolyte as indicated.

electrolytes with $\text{pH} > 10$ caused the dissociation of sulfonate groups, resulting in negative zeta potentials (Figure 5b, red circles). The key trend in Figure 5b for the amine PS particles is that both positively and negatively charged PS exhibited maximal aggregation rates when the zeta potential magnitude was minimal. Conversely, particles separated when the magnitude of the zeta potential was large, regardless of the pH or the sign of the zeta potential.

Several points about the observed zeta potential dependence are noteworthy. First, although there is clearly a correlation with the zeta potential, the observed aggregation does not depend solely on the zeta potential: there are many instances of similar zeta potentials yielding aggregation rates that differ by more than a factor of 2 (e.g., KCl and KBr for either silica or the amine PS). This observation indicates that other electrolyte-dependent parameters must also affect the aggregation rates. Second, we emphasize that k_E reflects a long-range interaction between particles separated by several particle radii, so the increasing tendency to separate with larger zeta potentials is not due to the classical electrostatic repulsion between charged double layers³¹ that decays on the Debye length scale (which is on the order of 10 nm here). Third, an increase in the aggregation rate with decreasing zeta potential is counterintuitive in the context of classical electrokinetic fluid flows, such as electroosmotic flow, which increases linearly with zeta potential for thin double layers.³¹ Some other mechanism that depends on the magnitude of the particle zeta potential must be operative.

The other significant correlation that we found was between the observed aggregation rate and the electric field strength

(Figure 6). Recall that all experiments for each particle size were performed at the same applied potential (5 V_{pp} for silica

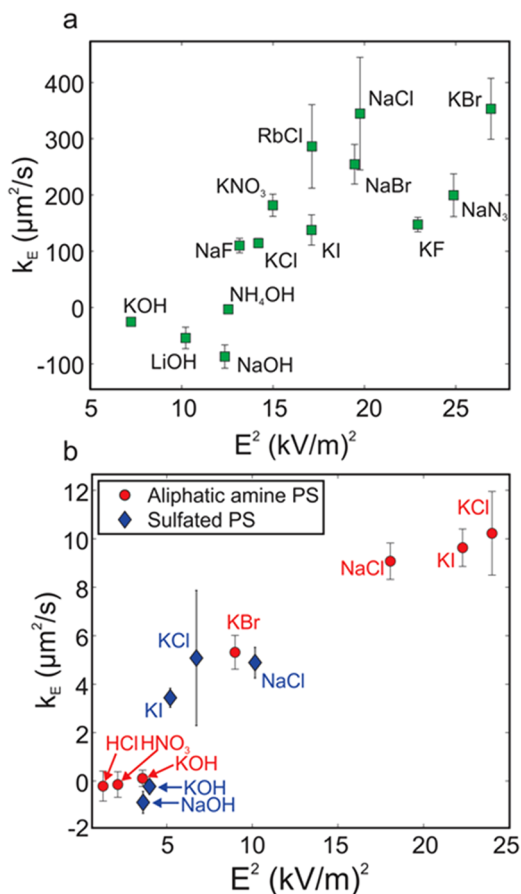


Figure 6. Aggregation rate, k_E , as a function of the electric field strength squared for (a) 4 μm silica particles and (b) 2 μm sulfated (blue diamonds) and aliphatic amine (red circles) PS.

and 2 V_{pp} for PS), so the varied field strengths reflect electrolyte-dependent differences in the observed current amplitude and ionic conductivity (cf. Table S1, noting $E = J/\sigma$ where J is the current density amplitude and σ is the electrical conductivity). As demonstrated in Figure 6, the clear trend is that electrolytes that yielded separation also had smaller measured electric fields than those of electrolytes that yielded aggregation. This trend is generally consistent with the idea that the aggregation is driven by an electrically generated fluid flow around the particles.

The strong electric field dependence of the aggregation rates suggests that the main contribution of the electrolyte is to set the electric field strength and thus the magnitude of the driving force that induces particle aggregation. It would be incorrect, however, to conclude that aggregation or separation is simply a function of exceeding a critical field strength. Importantly, previous work has established that higher applied potentials (and hence higher field strengths) do increase the rate of aggregation for particles in electrolytes such as KCl and NaCl,^{11,18} but increasing the applied potential for particles suspended in electrolytes such as NaOH and KOH does not cause them to aggregate; instead, they simply separate more rapidly.¹⁴ Our qualitative observations here confirm this: increasing the applied potential for particles immersed in KOH, for example, simply induced more rapid separation.

Because earlier investigations have shown that the aggregation rate for particles in an aggregating electrolyte (KCl) scales as E^2 ,^{11,32} we have likewise plotted the aggregation rates versus E^2 in Figure 6. The correlation coefficients (Pearson's product-moment correlation coefficient for linearity) are $R = 0.78$ for the silica particles and $R = 0.95$ for the PS particles. Almost identical correlation coefficients, however, of $R = 0.79$ for the silica particles and $R = 0.96$ for the PS particles were observed when correlating the aggregation rate versus E rather than E^2 (not shown). In other words, the general increase in aggregation rate with electric field strength is clear, but there is too much scatter in the data to differentiate between a linear or quadratic dependence on the field strength.

One possible hypothesis to explain the electrolyte dependence is the existence of a balance between attractive EHD fluid flow and repulsive induced dipolar forces. We tested our data against the point-dipole EHD model developed by Ristenpart et al.,¹¹ which was shown to capture the electric field and frequency dependence for particles immersed in KCl. In brief, the scaling analysis postulates that the fluid flow is driven by an electrical body force induced on the free charge near the electrode by the tangential component of the particle dipole field. To calculate the dipole field strength of the colloidal particle, we used the Hinch model to calculate the polarization properties of the particles in a low-frequency oscillatory electric field (Figure S2).³⁰ The attractive EHD flow for each electrolyte–particle combination was then balanced with a repulsive induced dipole–dipole force. The full details of the calculations are included in the Supporting Information.

When testing our electrolyte-dependent aggregation rates against the point-dipole model, however, we found that the predicted aggregation rate actually increased rather than decreased with the particle zeta potential (Figure S3). In other words, the point dipole model appears to capture the electric field and frequency dependence^{11,18} but fails to explain the observed dependence on zeta potential and electrolyte. One possible interpretation is that the Hinch model, which assumes an isolated particle with a thin double layer,³⁰ yields a poor representation of the dipole field around a particle in close proximity to an electrode surface with an oscillating free charge layer. Another possibility is that another type of electrically generated fluid flow, such as those proposed by Sides and Prieve and co-workers,^{12,16} is operative. A full test against their proposed mechanisms would require measurements of the phase angle between the oscillating particle height and oscillating electric field, measurements which are not available for the data collected here. In either case, more detailed numerical calculations of both the flow and particle dipole fields, which specifically incorporate the finite size of the particles and their proximity to the electrode and each other, are necessary to yield more accurate predictions of the particle behavior.

SUMMARY

We performed a broad survey of the effect of electrolyte type on the aggregation behavior of micrometer-scale colloidal particles near electrodes. Systematic tests of 26 distinct electrolyte–particle combinations revealed that the aggregation rate was negatively correlated with the magnitude of the particle zeta potential and positively correlated with the electric field strength. Although these results shed new light on the electrolyte dependence, the underlying mechanism remains unclear. We tested the experimental aggregation rates against

an EHD scaling model and found that our observations could not be reconciled with a force balance between induced dipolar repulsion and attractive drag force due to EHD flow, at least when using a point-dipole model for an isolated particle. Numerical modeling of the particle dipole coefficients that includes the finite size of the particle and its interaction with the electrode is necessary to determine whether the EHD scaling model will in fact describe electrolyte-dependent aggregation. We anticipate that this broad survey of electrolyte-dependent particle aggregation and separation provides a large data set against which future proposed models can be tested. Likewise, although the work here focused on silica and polystyrene particles at 100 Hz, the results are expected to shed light on the behavior of more complicated systems where the type of electrolyte might affect the response of particles to the applied electric field, including, for example, the EHD separation of vesicles^{33,34} or cells,^{35,36} order–disorder transitions in colloidal packing at low frequencies,¹⁸ and the assembly of metallic nanoparticles.³⁷

■ ASSOCIATED CONTENT

■ Supporting Information

A table of particle and electrolyte properties, a plot of representative ac electric fields, and the EHD scaling analysis and related plots. This material is available free of charge via the Internet at <http://pubs.acs.org>.

■ AUTHOR INFORMATION

Corresponding Author

*E-mail: wdristenpart@ucdavis.edu.

Present Addresses

T.J.W.: Division of Materials Science & Engineering, Ames Laboratory, Ames, Iowa 50014, United States.

C.S.D.: Department of Mechanical Engineering, University of Minnesota, Minneapolis, Minnesota 55455, United States.

Notes

The authors declare no competing financial interest.

■ ACKNOWLEDGMENTS

We thank the CA League of Food Processors and the UC Davis Academic Senate for supporting this research, and we thank Yifan Wang for experimental assistance.

■ REFERENCES

- (1) Richetti, P.; Prost, J.; Barois, P. Two-dimensional aggregation and crystallization of a colloidal suspension of latex spheres. *J. Phys. Lett.* **1984**, *45*, 23.
- (2) Trau, M.; Saville, D. A.; Aksay, I. A. Field-induced layering of colloidal crystals. *Science* **1996**, *272* (5262), 706–709.
- (3) Bohmer, M. In situ observation of 2-dimensional clustering during electrophoretic deposition. *Langmuir* **1996**, *12* (24), 5747–5750.
- (4) Trau, M.; Saville, D. A.; Aksay, I. A. Assembly of colloidal crystals at electrode interfaces. *Langmuir* **1997**, *13* (24), 6375–6381.
- (5) Yeh, S. R.; Seul, M.; Shraiman, B. I. Assembly of ordered colloidal aggregates by electric-field-induced fluid flow. *Nature* **1997**, *386* (6620), 57–59.
- (6) Sides, P. J. Electrohydrodynamic particle aggregation on an electrode driven by an alternating electric field normal to it. *Langmuir* **2001**, *17* (19), 5791–5800.
- (7) Gong, T.; Marr, D. W. M. Electrically switchable colloidal ordering in confined geometries. *Langmuir* **2001**, *17* (8), 2301–2304.

(8) Gong, T. Y.; Wu, D. T.; Marr, D. W. M. Two-dimensional electrohydrodynamically induced colloidal phases. *Langmuir* **2002**, *18* (26), 10064–10067.

(9) Kim, J.; Anderson, J. L.; Garoff, S.; Sides, P. J. Effects of zeta potential and electrolyte on particle interactions on an electrode under ac polarization. *Langmuir* **2002**, *18* (14), 5387–5391.

(10) Ristenpart, W. D.; Aksay, I. A.; Saville, D. A. Electrically guided assembly of planar superlattices in binary colloidal suspensions. *Phys. Rev. Lett.* **2003**, *90*, 12.

(11) Ristenpart, W. D.; Aksay, I. A.; Saville, D. A. Assembly of colloidal aggregates by electrohydrodynamic flow: Kinetic experiments and scaling analysis. *Phys. Rev. E* **2004**, *69*, 2.

(12) Fagan, J. A.; Sides, P. J.; Prieve, D. C. Mechanism of rectified lateral motion of particles near electrodes in alternating electric fields below 1 kHz. *Langmuir* **2006**, *22* (24), 9846–9852.

(13) Hoggard, J. D.; Sides, P. J.; Prieve, D. C. Electrolyte-dependent pairwise particle motion near electrodes at frequencies below 1 kHz. *Langmuir* **2007**, *23* (13), 6983–6990.

(14) Hoggard, J. D.; Sides, P. J.; Prieve, D. C. Electrolyte-dependent multiparticle motion near electrodes in oscillating electric fields. *Langmuir* **2008**, *24* (7), 2977–2982.

(15) Prieve, D. C.; Sides, P. J.; Wirth, C. L. 2-D assembly of colloidal particles on a planar electrode. *Curr. Opin. Colloid Interface Sci.* **2010**, *15* (3), 160–174.

(16) Wirth, C. L.; Rock, R. M.; Sides, P. J.; Prieve, D. C. Single and Pairwise Motion of Particles near an Ideally Polarizable Electrode. *Langmuir* **2011**, *27* (16), 9781–9791.

(17) Wirth, C. L.; Sides, P. J.; Prieve, D. C. Electrolyte dependence of particle motion near an electrode during ac polarization. *Phys. Rev. E* **2013**, *87* (3), 032302.

(18) Dutcher, C. S.; Woehl, T. J.; Talken, N. H.; Ristenpart, W. D. Hexatic-to-Disorder Transition in Colloidal Crystals Near Electrodes: Rapid Annealing of Polycrystalline Domains. *Phys. Rev. Lett.* **2013**, *111* (12), 128302.

(19) Bazant, M. Z.; Squires, T. M. Induced-charge electrokinetic phenomena: Theory and microfluidic applications. *Phys. Rev. Lett.* **2004**, *92* (6), 066101.

(20) Squires, T. M.; Bazant, M. Z. Induced-charge electro-osmosis. *J. Fluid Mech.* **2004**, *509*, 217–252.

(21) Bazant, M. Z.; Squires, T. M. Induced-charge electrokinetic phenomena. *Curr. Opin. Colloid Interface Sci.* **2010**, *15* (3), 203–213.

(22) Ristenpart, W. D.; Aksay, I. A.; Saville, D. A. Electrohydrodynamic flow around a colloidal particle near an electrode with an oscillating potential. *J. Fluid Mech.* **2007**, *575*, 83–109.

(23) Kim, J.; Guelcher, S. A.; Garoff, S.; Anderson, J. L. Two-particle dynamics on an electrode in ac electric fields. *Adv. Colloid Interface Sci.* **2002**, *96* (1–3), 131–142.

(24) Fagan, J. A.; Sides, P. J.; Prieve, P. C. Vertical oscillatory motion of a single colloidal particle adjacent to an electrode in an ac electric field. *Langmuir* **2002**, *18* (21), 7810–7820.

(25) Fagan, J. A.; Sides, P. J.; Prieve, D. C. Vertical motion of a charged colloidal particle near an AC polarized electrode with a nonuniform potential distribution: Theory and experimental evidence. *Langmuir* **2004**, *20* (12), 4823–4834.

(26) Fagan, J. A.; Sides, P. J.; Prieve, D. C. Evidence of multiple electrohydrodynamic forces acting on a colloidal particle near an electrode due to an alternating current electric field. *Langmuir* **2005**, *21* (5), 1784–1794.

(27) Zhang, K.-Q.; Liu, X. Y. Controlled formation of colloidal structures by an alternating electric field and its mechanisms. *J. Chem. Phys.* **2009**, *130* (18), 184901.

(28) Ma, F. D.; Wang, S. J.; Smith, L.; Wu, N. Two-Dimensional Assembly of Symmetric Colloidal Dimers under Electric Fields. *Adv. Funct. Mater.* **2012**, *22* (20), 4334–4343.

(29) Ma, F. D.; Wu, D. T.; Wu, N. Formation of Colloidal Molecules Induced by Alternating-Current Electric Fields. *J. Am. Chem. Soc.* **2013**, *135* (21), 7839–7842.

(30) Hinch, E. J.; Sherwood, J. D.; Chew, W. C.; Sen, P. N. Dielectric response of a dilute suspension of spheres with thin double-layers in an

asymmetric electrolyte. *J. Chem. Soc., Faraday Trans. 2* **1984**, *80*, 535–551.

(31) Russel, W. B.; Saville, D. A.; Schowalter, W. R. *Colloidal Dispersions*; Cambridge University Press: Cambridge, U.K., 1991.

(32) Vigo, C. R.; Ristenpart, W. D. Aggregation and Coalescence of Oil Droplets in Water via Electrohydrodynamic Flows. *Langmuir* **2010**, *26* (13), 10703–10707.

(33) Lecuyer, S.; Ristenpart, W. D.; Vincent, O.; Stone, H. A. Electrohydrodynamic size stratification and flow separation of giant vesicles. *Appl. Phys. Lett.* **2008**, *92*, 10.

(34) Ristenpart, W. D.; Vincent, O.; Lecuyer, S.; Stone, H. A. Dynamic Angular Segregation of Vesicles in Electrohydrodynamic Flows. *Langmuir* **2010**, *26* (12), 9429–9436.

(35) Zhou, H.; White, L. R.; Tilton, R. D. Lateral separation of colloids or cells by dielectrophoresis augmented by AC electroosmosis. *J. Colloid Interface Sci.* **2005**, *285* (1), 179–191.

(36) Bhatt, K. H.; Grego, S.; Velev, O. D. An AC electrokinetic technique for collection and concentration of particles and cells on patterned electrodes. *Langmuir* **2005**, *21* (14), 6603–6612.

(37) Song, M.-G.; Bishop, K. J. M.; Pinchuk, A. O.; Kowalczyk, B.; Grzybowski, B. A. Formation of Dense Nanoparticle Monolayers Mediated by Alternating Current Electric Fields and Electrohydrodynamic Flows. *J. Phys. Chem. C* **2010**, *114* (19), 8800–8805.